

Irfan Khan¹, Siti Maisurah Mohd Hassan², Mardeni Roslee^{*1}, Farman Ali¹, Yasir Ullah¹, Fardin Kabir¹

¹ Faculty of AI & Engineering, Multimedia University, Cyberjaya 63100, Malaysia

² Center for Intelligent Network, Telekom Malaysia R&D, Cyberjaya 63100, Malaysia

Email: irfanbehlol@gmail.com, maisurah@tmrmd.com.my, mardeni.roslee@mmu.edu.my, farmanali@mmu.edu.my, yasirullah415@gmail.com, fardinkabirr@gmail.com

Corresponding Author: Mardeni Roslee*

ABSTRACT:

Unmanned Aerial Vehicles (UAVs) are increasingly used in wireless networks because of their ability to provide mobility and wide range coverage. However, the reliable UAV-to-Ground (U2G) communication in Future Wireless Networks (FWNs), remains challenging. The main difficulties arise from UAV posture changes during flight, the presence of static and dynamic scatterers in dense environments, and the frequency-selective nature of fading across different bands. The existing models focus on simplifying these factors, which limit their accuracy. This paper proposes a posture-aware, multi-modal, and frequency-selective channel modeling framework for U2G communication. The framework includes UAV yaw, pitch, and roll to capture posture effects on multipath behavior and Doppler spread. It also combines LiDAR sensing with Radiofrequency (RF) data to distinguish between static and dynamic scatterers. In addition, Graph Neural Network (GNN) and Grasshopper Optimization Algorithm (GOA) are used to learn spatial-temporal channel features and optimize delay spread, coherence bandwidth, and angular dispersion across sub-6 GHz and mm Wave bands. The simulation results indicate reduced Path Loss Root Mean Square Error (PL-RMSE) and more accurate predictions of delay spread and coherence bandwidth across sub-6 GHz and mm Wave bands.

KEYWORDS:

Channel Modeling, Frequency-Selective Fading, FWNs, GNN, GOA, LiDAR Integration, Multi-Modal Sensing, Introduction

Unmanned Aerial Vehicles (UAVs) are becoming a vital part of modern wireless communication because they offer mobility, flexibility, and wide coverage in urban areas [1]. Reliable UAV-to-Ground (U2G) links, particularly in Future Wireless Networks (FWNs), are essential for applications such as emergency response, smart cities, and real-time monitoring [2], [3]. However, creating accurate channel models for these links is still unexplored and insufficiently validated [4], [5]. The main challenges come from posture changes of the UAV during flight, the presence of static and dynamic scatterers in dense environments, and the frequency-selective nature of fading [6].

Several research works have addressed these issues from different angles but with certain limitations. Geometry-based stochastic models describe large- and small-scale fading, but they often simplify the environment and do not use sensing data [7]. Multi-modal approaches combine LiDAR and RF signals to identify scatterers, though they typically ignore posture changes and frequency-selective fading [8]. Analytical studies have focused on altitude and elevation to optimize coverage [9], while other works modeled the effect of UAV position fluctuations and blockages in mm Wave bands [10]. Machine learning has been used for clustering and multipath tracking, and measurement-driven models have examined vegetation penetration loss [12] or fading behavior in OFDM-based systems [12]. Our earlier work introduced a frequency-aware U2G model using a GNN and GOA, which improved prediction accuracy across multiple bands. Yet, posture dynamics, multi-modal sensing, and unified frequency-selective modeling remain largely unexplored.

Accurate U2G channel modeling requires these factors to be considered together rather than separately. UAV posture changes, such as yaw, pitch, and roll, can alter angular dispersion and Doppler spread. Ignoring dynamic scatterers like vehicles or pedestrians underestimates the variability of the urban channel, while frequency-selective fading across sub-6 GHz and mm Wave bands requires models that adapt to multiple spectral conditions. Without addressing these combined effects, channel models remain limited in realism and predictive power. These challenges motivate a unified framework that integrates posture awareness, multi-modal sensing, and frequency-selective learning into a single approach. **This paper addresses these gaps by proposing a posture-aware, multi-modal, frequency-selective channel modeling framework for U2G communication in urban environments. The key contributions are as follows: Firstly, we explicitly model UAV yaw, pitch, and roll to quantify their impact on multipath clustering, Doppler spread, and angular dispersion.**

Secondly, we use LiDAR sensing with RF measurements to distinguish static and dynamic scatterers, leading to a more realistic representation of dense urban propagation. Finally, we develop a Graph Neural Network (GNN) and Grasshopper Optimization Algorithm (GOA) pipeline to learn spatio-temporal features from the Channel Impulse Response (CIR) and to optimize delay spread, coherence bandwidth, and angular dispersion across sub-6-GHz and mm Wave bands.

- 1. System Model:** The proposed system model in figure-1 shows how posture, LiDAR sensing, and frequency diversity work together in the U2G channel. The UAV sends signals toward the ground users through both LoS and NLoS paths, while LiDAR maps the scene to detect static and moving objects. The UAV's posture (yaw, pitch, and roll) changes the direction of the antenna, which alters reflection and Doppler effects. Multiple frequencies from 3.5 GHz to 39 GHz are used to study how propagation changes across sub-6 GHz and mm Wave bands. The combination of LiDAR sensing and posture-aware modeling allows the system to identify clear, blocked, and scattered paths, giving a more realistic and data-driven view of U2G communication in complex urban areas.

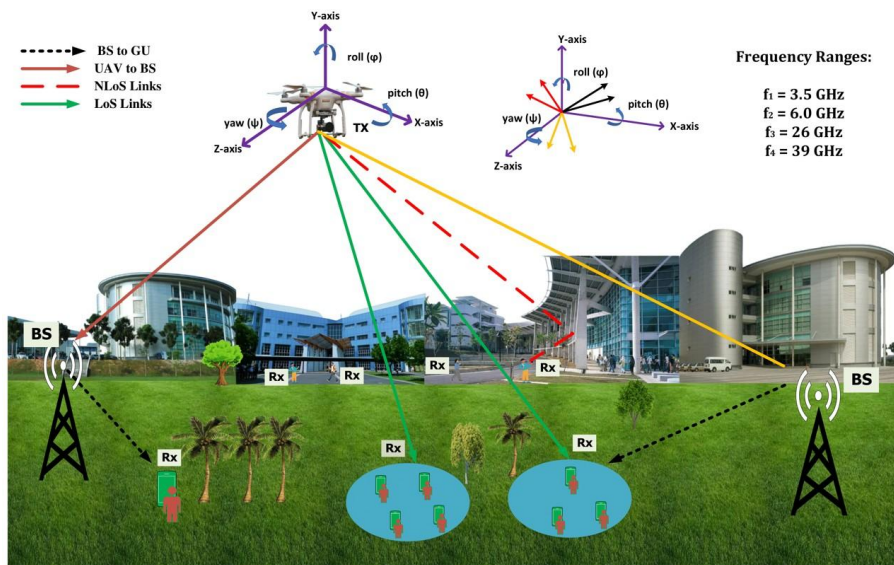


Figure 1 Proposed System Model

Figure 2 illustrates the flow for our proposed posture- and LiDAR-aware U2G model. We first take the inputs, including UAV altitude, 3D orientation (yaw, pitch, roll), trajectory, ground-user position, carrier frequency, and environments type. From these, we compute the distance between Tx–Rx and the elevation angle. These two values determine the antenna gains and the large-scale PL. Next, we utilize LiDAR to generate a visibility mask to assess LoS, NLoS, or blocked, and it identifies scatterers as static or dynamic. With this assessment, we build the CIR and add LoS, static-NLoS, and dynamic-NLoS taps. Furthermore, we include phase and Doppler from posture. For large-scale fading, we use a dual-slope PL model with log-normal shadowing and keep shadowing consistent in space with an exponential correlation. Moreover, a GNN with GOA optimizes the key parameters $\{L_0, \gamma, \sigma, \tau_{rms}, B_c\}$, so the simulated results match the data. Finally, the outputs support beamforming, link-budget evaluation, delay-spread and coherence-bandwidth analysis, and throughput estimation.

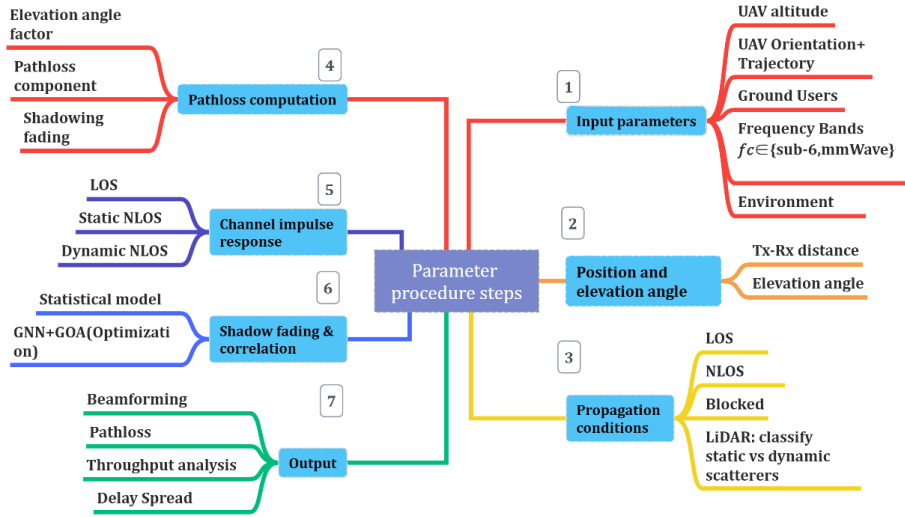


Figure 2 Parameter procedure steps

2. **Mathematical Modeling and Formulation:** This section presents the mathematical formulation of the proposed posture-aware, multi-modal, frequency-selective U2G channel model. The model integrates UAV posture dynamics, LiDAR-based environmental sensing, and frequency-selective channel learning to capture the complex spatial-temporal behavior of U2G propagation in dense environments.

• **Posture-Aware Geometry and Kinematics**

The UAV position and orientation are represented in the 3D Cartesian coordinate system as:

$$\mathbf{p}_t(t) = [x_t(t), y_t(t), z_t(t)]^T, \quad \mathbf{p}_r = [x_r, y_r, z_r]^T \quad (1)$$

Where $\mathbf{p}_t(t)$ and \mathbf{p}_r denote the transmitter (UAV) and ground receiver positions, respectively. The UAV posture is defined by three rotational angles: yaw (ψ), pitch (θ), and roll (ϕ).

The combined rotation matrix is expressed as:

$$\mathbf{R}(t) = \mathbf{R}_z(\psi)\mathbf{R}_y(\theta) \mathbf{R}_x(\phi), \quad (2)$$

Where $\mathbf{R}_z(\psi)\mathbf{R}_y(\theta)\mathbf{R}_x(\phi)$, are the rotation matrices about the x, y and z axes, respectively.

The 3D link distance and direction unit vector between the UAV and ground user are:

$$d_{3D}(t) = \|\mathbf{p}_t(t) - \mathbf{p}_r\|_2, \quad \mathbf{u}(t) = \frac{\mathbf{p}_r - \mathbf{p}_t(t)}{d_{3D}(t)}. \quad (3)$$

The elevation and azimuth angles at the receiver are then obtained as:

$$\alpha(t) = \arcsin(\hat{u}_z(t)), \quad \beta(t) = \tan^{-1}\left(\frac{\hat{u}_y(t)}{\hat{u}_x(t)}\right). \quad (4)$$

• **LiDAR-RF Multi-Modal Sensing Integration**

The LiDAR sensor continuously maps the surrounding environment to detect both static and dynamic scatterers. Let S_s and S_d denote the sets of static and dynamic scatterers, respectively. For each detected scatterer \mathbf{m} , an occlusion mask $O_m(f, t) \in \{0, 1\}$ is applied such that $O_m(f, t) = 0$ if the path is blocked.

The complex amplitude for the m-th path is defined as:

$$a_m(f, t) = O_m(f, t)G_T(\Omega_{t,m}, t)G_R(\Omega_{r,m}) [-2pt] \times g_m(f)\ell_m^{-1}(f, t), a_m(f, t) = O_m(f, t)G_T(\Omega_{t,m}, t)G_R(\Omega_{r,m}) [-2pt] \times g_m(f)\ell_m^{-1}(f, t),$$

Where G_T and G_R represent the antenna pattern gains, $g_m(f)$ the scattering coefficient, and $\ell_m(f, t)$ the geometric attenuation factor.

• **Time-Varying Channel Impulse Response**

The overall U2G CIR is expressed as

$$h(t) = \alpha_{LoS}e^{-j2\pi f_c \tau_{LoS}(t)} + \sum_{i \in S_s} \alpha_i e^{-j2\pi f_c \tau_i(t)} + \sum_{j \in S_d} \beta_j(t) e^{-j2\pi f_c \tau_j(t)} e^{j2\pi f_{D,j}(t)t}, \quad (6)$$

Where $\tau_i(t)$ is the propagation delay, $\beta_j(t)$ is the time-varying reflection coefficient, and $f_{D,j}(t)$ represents the Doppler shift induced by UAV and scatterer motion.

For wideband modeling, the frequency-domain response is given by

$$H(f, t) = \sum_m a_m(f, t) e^{-j2\pi f \tau_m(t)} e^{j2\pi f_{D,m}(t)t} \quad (7)$$

- **Path-Loss and Shadow Fading Modeling**

The PL component is modeled using a dual-slope function with elevation dependency,

$$PL(d, f) = L_0(f) + 10\gamma_1(f) \log_{10} \left(\frac{d}{d_0} \right) + X_\sigma, \quad d \leq d_{BP}, [4pt] L_0(f) + 10\gamma_1(f) \log_{10} \left(\frac{d_{BP}}{d_0} \right) + 10\gamma_2(f) \log_{10} \left(\frac{d}{d_{BP}} \right) + X_\sigma, \quad d > d_{BP}, \quad (8)$$

Where $L_0(f)$ is the reference loss, $\gamma_1(f)$ and $\gamma_2(f)$ are the near- and far-field exponents, d_{BP} is the breakpoint distance, and $X_\sigma \sim N(0, \sigma^2)$ models log-normal shadowing.

The shadowing spatial correlation is characterized as

$$\rho(\Delta r) = \exp \left(- \frac{\|\Delta r\|}{d_{cor}} \right), \quad (9)$$

Where d_{cor} is the decorrelation distance.

- **Frequency-Selective Statistics**

The Power Delay Profile (PDP) is defined as

$$P(\tau, t) = E_f \{ |h(\tau, t)|^2 \} \quad (10)$$

and the root-mean-square (RMS) delay spread is obtained by

$$\tau_{rms} = \sqrt{\frac{\int (\tau - \bar{\tau})^2 P(\tau) d\tau}{\int P(\tau) d\tau}}, \quad \bar{\tau} = \frac{\int \tau P(\tau) d\tau}{\int P(\tau) d\tau}. \quad (11)$$

The coherence bandwidth is approximated as

$$B_c^{(0.5)} \approx \frac{1}{5\tau_{rms}}, \quad B_c^{(0.9)} \approx \frac{1}{50\tau_{rms}} \quad (12)$$

- **Learning and Optimization via GNN-GOA**

To improve modeling accuracy across frequency bands, a hybrid learning scheme integrates a GNN and the GOA. The GNN predicts initial parameters $\{L_0, \gamma, \sigma, \tau_{rms}, B_c\}$ from posture, LiDAR, and geometric features, while GOA refines these parameters to minimize mean-square error (MSE) between simulated and measured data.

$$\min_{\Theta(f)} \sum_{f \in F} \left[\frac{1}{N} \sum_n (PL_\Theta(d_n, f) - PL^{meas}(d_n, f))^2 [3pt] + \kappa_1 \left| \tau_{rms, \Theta}(f) - \tau_{rms}^{meas}(f) \right| + \kappa_2 \left| B_{c, \Theta}(f) - B_c^{meas}(f) \right| \right]. \quad (13)$$

GOA updates each agent's position vector according to,

$$\mathbf{x}_i^{t+1} = \mathbf{x}_i^t + c(t) \sum_{j \neq i} s(\|\mathbf{x}_j^t - \mathbf{x}_i^t\|) \frac{\mathbf{x}_j^t - \mathbf{x}_i^t}{\|\mathbf{x}_j^t - \mathbf{x}_i^t\|} + \mathbf{T}_d \quad (14)$$

Where $c(t)$ is a linearly decreasing coefficient, $s(\cdot)$ is the comfort function controlling attraction/repulsion, and \mathbf{T}_d is the target drift term.

3. Results and Discussion

The proposed posture-aware, LiDAR-fused, and frequency-selective U2G channel model was simulated using MATLAB 2024b in an urban scenario reconstructed from LiDAR point clouds. The simulation integrates UAV posture dynamics (yaw, pitch, roll) with multi-frequency propagation modeling at 3.5, 6, 26, and 39-GHz. LiDAR data are used to classify static and dynamic scatterers, enabling geometry-aware visibility and occlusion analysis. The integration of

GNN-GOA algorithms optimizes model parameters $\{L_0, \gamma, \sigma\}$ for each frequency band to minimize the RMSE between predicted and measured PL. The detailed simulation configuration is summarized in Table 1.

Parameters	Values/Description
Simulation platform	MATLAB 2024b
Environment	LiDAR-based urban mesh 1km ²
Frequency bands	3.5, 6, 26, 39-GHz
Bandwidths	100, 160, 400, 1000-MHz \
UAV altitude	30-120m
UAV velocity	5-20 m/s
Posture angles	$Yaw \pm 45^\circ, Pitch \pm 10^\circ, Roll \pm 15^\circ$
Receiver height	1.5m
LiDAR resolution	0.2 m spacing, 10 Hz frame rate
Scatterers	$N_s = 60$ static, $N_d = 20$ dynamic
Optimization	GNN prediction with GOA refinement
Evaluation metrics	PL RMSE, τ_{rms} , B_c , Doppler PSD

Table: List of Simulation Parameters

Figure 3 demonstrates RMS delay spread versus carrier frequency at altitudes of 40, 80, and 120 m and shows that how RMS delay spread changes with frequency and altitude. The delay spread decreases as frequency increases because at higher bands high probability of NLoS paths, and vice versa. The error bars shrink at higher frequency and altitude because the channel becomes more stable and fewer reflectors contribute. The posture of the UAV affects the spread more at low altitude because environmental obstacles create wider angular and delay spreads. The LiDAR gating explains the drop at high frequency because the sensor removes blocked and weak paths before modeling. The GNN-GOA explains the tighter trends because the optimizer tunes PL and clustering parameters to match measurements. The combined evidence supports our model because both frequency and altitude push the U2G link toward a LoS-dominant regime with larger coherence bandwidth.

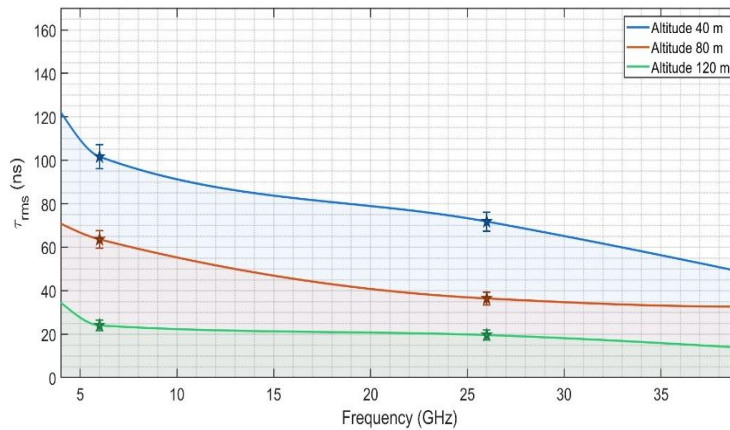


Figure 3 RMS delay spread vs. frequency bands.

Similarly, Figure 4 shows how the RMS delay spread changes with UAV altitude at four different carrier frequencies. The delay spread decreases steadily as the UAV altitude increases, showing that higher flight levels reduce the number of reflected and diffracted paths. This reduction occurs because the UAV maintains a clearer LoS link at higher altitudes, minimizing multipath distortion.

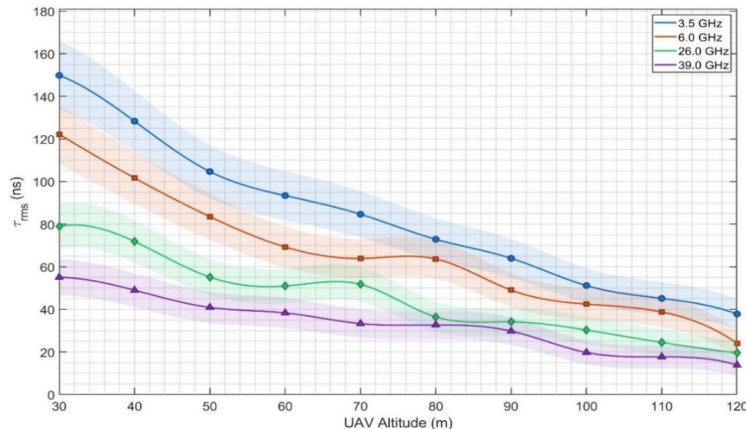


Figure 4 RMS delay spread vs. altitude across frequency bands.

At lower altitudes, buildings and vehicles contribute to stronger scattering, which increases the delay spread. Across all altitudes, the delay spread is smaller at higher frequencies, which are more sensitive to blockage and less capable of penetrating obstacles. The shaded regions indicate variability caused by dynamic scatterers detected by LiDAR, which becomes less significant at higher altitudes. Overall, the trend confirms that both altitude and frequency strongly influence time dispersion, and the proposed posture- and LiDAR-aware model effectively captures these variations in complex urban environments.

Furthermore, Figure 5 validates the proposed GNN-GOA scheme and its post-optimization improvements across multiple frequency bands. On the left, it shows the feature-to-parameter mapping, where posture, LiDAR, geometry, and band features are processed by the GNN to predict key channel parameters. The GOA stage then refines these parameters to minimize prediction error and improve generalization. On the right, the heatmap quantifies performance gains, showing consistent improvement with increasing frequency. Overall, the combined GNN-GOA approach enhances parameter convergence and achieves higher accuracy in multi-band U2G channel prediction.

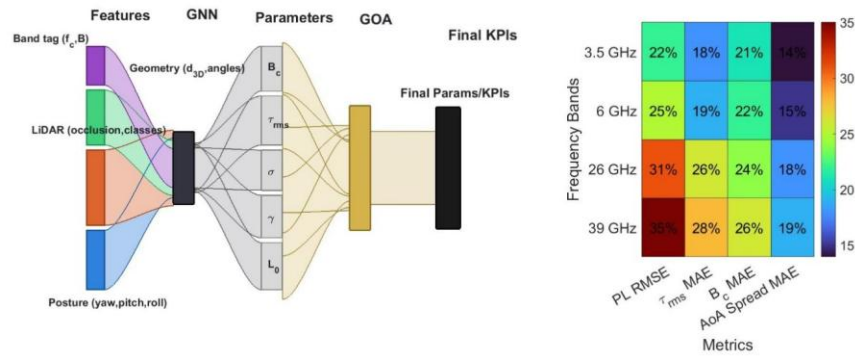


Figure 5 GNN-GOA pipeline visualization (heatmap)

4. Conclusion

This paper presented a posture-aware, multi-modal, and frequency-selective U2G channel model that fuses LiDAR with RF data and learns key parameters through GNN–GOA integration. The model captures how yaw, pitch, and roll shape multipath, Doppler, and angular spreads, and it improves PL and delay-spread prediction across various frequency bands. The simulation results demonstrate that at higher frequencies and altitudes, the proposed approach reduces delay spread and moves the link toward LoS dominance, which supports more reliable UAV links in FWNs. In future, we will validate the model with large-scale field trials, extend it to polarization-aware MIMO and RIS-assisted links, and evaluate its generalization across diverse and ultra-dense urban environments as well as heterogeneous UAV platforms.

Acknowledgement: This work was supported and funded by a Telekom Malaysia Research and Development (TMR&D) grant, MMUE/240087, RDTC/241139, Malaysia.

References:

- [1] He, Dongxuan, et al. "Ubiquitous UAV Communication Enabled Low-Altitude Economy: Applications, Techniques, and 3GPP's Efforts." *IEEE Network* (2025).
- [2] Ullah, Yasir, et al. "DDPG-based UAV-RIS framework for optimizing mobility in future wireless communication networks." *Drones* 9.6 (2025): 437.
- [3] Y. Ullah, M. Roslee, M. Z. Fadli, J. M. L. Jayakanthan, F. Ali, I. Khan, and F. Kabir, "A review on mobility and handover management in future wireless networks," *TPM – Testing, Psychometrics, Methodology in Applied Psychology*, vol. 32, no. S6, pp. 1590–1595, Sep. 2025.
- [4] F.-Li, X.-Ge, J.-Zhang, and J.-Li, "Ultra-wideband nonstationary channel modeling for UAV-to-ground communications," *IEEE Access*, vol. 7, pp. 117460–117471, Aug. 2019.
- [5] Sharma, Geeta, Sanjeev Jain, and Radhe Shyam Sharma. "Path planning for fully autonomous UAVs-a taxonomic review and future perspectives." *IEEE Access* (2025).
- [6] Pengyu, Dong, et al. "A robust MMSE-DFE framework with joint time-frequency domain processing for UAV-to-ground SC-FDE communication systems." *Wireless Networks* (2025): 1-20.
- [7] Yang, Xiaobo, et al. "A Geometry-Based Stochastic Channel Model for UAV-to-Ground Integrated Sensing and Communication Scenarios." *IEEE Transactions on Vehicular Technology* (2024).
- [8] Bai, Lu, et al. "A Multi-Modal UAV-to-Ground Channel Model for 6G Intelligent Sensing-Communication Integration." *IEEE Transactions on Communications* (2025).
- [9] Lala, Valencia, et al. "Channel Modelling for UAV Air-to-Ground Communication." 2024 5th International Conference on Emerging Trends in Electrical, Electronic and Communications Engineering (ELECOM). IEEE, 2024.
- [10] Ma, Cunyan, et al. "Effects of UAV Position Fluctuations on Air-to-Ground mm Wave UAV Communications with Multiple Types of Blockages." *IEEE Transactions on Intelligent Transportation Systems* 99 (2025): 1-15.
- [11] Zhang, Zhaolei, et al. "Machine learning based clustering and modeling for 6G UAV-to-ground communication channels." *IEEE Transactions on Vehicular Technology* 73.10 (2024): 14113-14126.
- [12] Zhu, Yiyong, and Yao Chen. "Modeling of UAV ground-air communication Channel based on OFDM system." 2022 IEEE International Conference on Unmanned Systems (ICUS). IEEE, 2022.